eurasia

Augmenting Antioxidative Properties of Cerium Oxide Nanomaterial with *Andrographis paniculata* Mediated Synthesis and Investigating its Biomedical Potentials

Article history:
Received: 12-11-2023
Revised: 05-02-2024
Accepted: 05-02-2024
Published: 21-04-2024

Sneha Kumari[a], ShivamPandey[b], Leela Manohar Aeshala[c], Anuj Kumar[d], Sushant Singh[e]

Abstract: Extensive interest has been poured into the production of sustainable nanomaterials. We report the fabrication of cerium oxide nanomaterial (CNP) utilizing crude extracts of *Andrographis paniculata*. This synthesis route devises a sustainable approach with the implementation of a less energy-intensive process and avoids hazardous chemicals. The crude extracts of *Andrographis paniculata (cAP)* act simultaneously as a reducing and stabilizing agent and support the nucleation of CNP leading to unique physiochemical properties. The cAP-CNP conjugate is found in the size range of 150 nm with signature UV peaks at 310 nm indicating Ce^{+4} surface oxidation state. Scanning electron microscope and X-ray diffraction analysis of cAP-CNP conjugate indicates the ultra-structure of dry powder and polycrystalline signature peaks with 111, 200, 220 and 311 crystal planes indicating pure cubic fluorite structure. Further cAP-CNP conjugate also reports high H_2O_2 (80%) and moderate superoxide anion (40%) antioxidative scavenging. The cAP-CNP nanomaterial conjugates exhibit excellent antimicrobial behavior with a reduction of 60% *E. coli* bacterial growth. Similarly, cAP-CNP conjugate exhibits alpha-amylase inhibition (80%) activity indicating its prospects in diabetics'management. *In-vitro* analysis results the biocompatibility with 85% skin keratinocyte cell growth. Anti-inflammatory assay revealed IL-6 (89%) and TNF-alpha (81%) reduced expression. Overall, cAP-CNP demonstrates a sustainable approach to prospective biomedical applications.

Keywords: Cerium Oxide Nanoparticle; *Andrographis paniculata;* Catalase; Antimicrobial; Antioxidative Nanoparticle.

[a] Amity Institute of Biotechnology, Amity University Chhattisgarh, Raipur - 493225, Chhattisgarh, India.

[b] Amity Institute of Biotechnology, Amity University Chhattisgarh, Raipur - 493225, Chhattisgarh, India.

[c] Department of Chemical Engineering, National Institute of Technology Warangal, Telangana-506004, India.

[d] School of Materials Science and Technology, Indian Institute of Technology (BHU), Varanasi 221005, India.

[e] Amity Institute of Biotechnology, Amity University Chhattisgarh, Raipur - 493225, Chhattisgarh, India.
Corresponding Author:
drssingh1983@gmail.com

1. INTRODUCTION

In the last decade, development in nanotechnology has revolutionized several sectors in terms of application including electronics, biomedical, energy and environmental applications. Cerium oxide nanoparticles (CNP), which are among the wide range of nanomaterials, have drawn a lot of interest owing to their exceptional physicochemical qualities, which include catalytic, optical, electrical and biomedical properties. CNP applications are highly applied in fuel cells, catalysis, sensors, solar cells, and drug delivery systems because of their unique redox nature (Khatami *et al.,* 2019; Miri & Sarani, 2018). However, the traditional synthesis technique often requires hazardous chemicals and energy-intensive processes have a negative influence on the

residual environment. Researchers are increasingly using eco-friendly and sustainable approaches for the production of nanoparticles to solve emerging environmental contamination issues. Utilization of a plant-based approach in nanomaterials development is one such strategy. The materials developed through these routes have a number of benefits including biocompatibility, cost-effectiveness, and minimal usage of hazardous effects (Smith *et al.*, 1996; Javadi *et al.,* 2019). *Andrographis paniculata*, generally referred to as the "King of Bitters," has emerged as a potential choice for the sustainable or green synthesis of CNP among the vast array of plants. Due to its numerous therapeutic benefits, *Andrographis paniculate* is one of the common medicinal plants utilized for traditional medicinal practices notably in the Asian region. Flavonoids, andrographolide, neoandrographolide and other bioactive chemicals found in the plant have antioxidant, anti-inflammatory, antibacterial and anticancerous properties (Singh *et al.*, 2016; Zou *et al.*, 2010). *Andrographis paniculate* plant is an excellent choice for the sustainable synthesis of nanoparticles with improved biological characteristics and reduced toxicity owing to its distinctive chemical components. With the help of crude extracts of *Andrographis paniculate* CNP can be fabricated with a sustainable approach. The extraction of bioactive constituents is facilitated by incorporating suitable solvent ratios such as deionized water, methanol, ethanol, etc. During the synthesis process, the phytoconstituents serve as a stabilizing and reducing agent simultaneously (Wu *et al.,* 2012; Cheung *et al.,* 2001). In comparison to traditional synthesis techniques, the synthesis of cAP-CNP conjugate utilizing phytoconstituent of *Andrographis paniculata* has several benefits including hazardous chemical-free, environmentally safe and eco-friendly manner. Additionally, this synthesis procedure is economically practical and scalable for large-scale manufacturing due to the plant's plentiful availability and cost-effectiveness. *Andrographis paniculate* has been reported for excellent biocompatibility, and reduced cytotoxicity of the synthesized nanoparticles, making them appropriate for biomedical applications (Chien *et al.,* 2010). The evolution of sustainable and green nanotechnology is aided by ongoing research and development, which also supports a sustainable and environmentally safe future (Saxena *et al.,* 2010). Herein, we demonstrate asustainable approach for the synthesis of redox-active cerium oxide nanomaterial using crude extracts of *Andrographis paniculata*, hereafter referred to as cAP-CNP conjugate. We anticipate this sustainable fabrication approach leads to highly redox active cAP-CNP nanomaterial synthesis with enhanced antioxidative scavenging properties. Additionally, we would also be testifying the synthesized material for the prospective biomedical potentials in antimicrobials and anti-inflammatory roles.

2. MATERIALS AND METHODS

2.1. Materials required

Cerium Nitrate Hexahydrate (Catalogue. No – GRM1441) from Hi-Media, *Andrographis paniculata* plant extract powder from Bixa Botanica (Approved by FDA), 30% H_2O_2 (Cat. No- PCT1511), Ascorbic acid (Cat. No- 01550, by Loba Chemie), Nitrobule Tetrazolium (NBT) (Cat. No. RM578 by Hi- Media), Methionine (Cat. No. PCT0315, by Hi-Media), LB Broth (Cat. No. G008, Make-Hi-Media), α-amylase (Cat. No. GRM638, Make-Hi-Media), starch (Cat. No. GRM424, Make-Hi-Media), Di-nitrosalicylic acid (Cat. No. 128848, Make-Sigmaldrich), and Acarbose (Cat. No. A8980, Make-Sigmaaldrich).

2.2. Synthesis of crude *Andrographis paniculata* and Cerium oxide Nanoparticles conjugate (cAP-CNP)

Cerium nitrate hexahydrate was used as a base source for the cerium oxide nanoparticle synthesis. A stoichiometric amount of Cerium nitrate hexahydrate was dissolved in 35 ml of distilled water, the solution was properly stirred until it turned crystal clear. Once the clear solution was obtained aqueous solution of plant extract (1mg/ml) was added to the solution and stirred to obtain a homogenized mixture of inter-fused nanomaterials. The obtained mixture was then further centrifuged at 4,000 rpm for refinement and the conjugation was confirmed by the last step of synthesis through calcination at 600 ºC for 40 minutes (Aseyd *et al.,* 2020). The crude extract of *Andrographis paniculata* was obtained *via* Soxhlet apparatus by using methanol as solvent. Following the same protocol, the bare CNP was obtained by using H_2O_2 as an oxidizer. The bare CNP and aqueous crude plant extract were used in the assessment of synergistic effects in the enhancement of biomedical properties of conjugated nanomaterial (cAP-CNP).

2.3. UV-visible, DLS, XRD, FTIR and SEM Characterization

The synthesized samples were characterized using UV-visible spectroscopy (UV-Vis) and dynamic light scattering (DLS). UV-Vis spectra were obtained using a Novostrix Nanodrop UV visible instrument. Confirmatory peaks were observed in between the range of 220-720 nm, which corresponded to the Ce^{4+} surface oxidation state. DLS was performed using a Litesizer 500 instrument. The distribution of size for the synthesized samples via analysis of hydrodynamic radius was determined to be between 50 and 250 nm. Samples were ultrasonicated for 15 minutes before analysis to ensure that particles were fully dispersed in the solution. The crystalline nature of the sample nanomaterial was studied through XRD technique and the planes obtained were used to define its crystalline configuration. FTIR was carried out using Shimadzu FTIR instrument for studying the functional groups present on the surface of nanomaterials to obtain better clarity regarding conjugation chemistry whereas SEM was performed regarding the surface morphology of the samples.

2.4. Antioxidative Catalytic Activity of cAP-CNP

Catalase activity was evaluated using a reaction mixture prepared with 30 µl of cAP-CNP, bare CNP, or plant extract, 50 mM sodium phosphate buffer, and 20 mM H_2O_2. The consumption of H_2O_2 was monitored at 15-minute intervals using spectrophotometry at 240 nm. The extent of H_2O_2 breakdown was determined by tracking the decline in absorbance over time (Mendes *et al.*, 2014). The superoxide dismutase (SOD) assay was conducted using the Nitro Blue Tetrazolium (NBT) reduction method. Three different tubes were used: Blank (B), Test (T), and Control (C). The Blank tube contained methionine, riboflavin, and phosphate buffer but no samples of cAP-CNP nanomaterials. The Test (T) tube contained the same ingredients as the Blank tube, plus cAP-CNP, bare CNP, or plant extract assessed separately for its potential SOD mimetic activity. The Control tube contained methionine, riboflavin, NBT, samples and phosphate buffer, but no LED treatment was provided (Weydert *et al.*, 2010; Singh *et al.*, 2021).

2.5. Antimicrobial and α-amylase inhibition analysis of cAP-CNP

To determine the concentration range of nanoparticles that inhibit bacterial growth, a stock solution of nanoparticles was diluted in sterile growth media. A fresh culture of *E. coli* was prepared and standardized to a desired cell density. The diluted nanoparticle solutions were added to test tubes, along with the standardized *E. coli* culture. The plates and tubes were incubated at 37ºC for 14 hours. The presence or absence of visible bacterial growth was then determined by examining the turbidity of broth solution and then the Optical Density was taken at 600 nm for assessment (Gahlaut & Chhillar, 2013; Ivanova *et al.*, 2013; Karuppusamy & Rajasekaran, 2009). Other biomedical efficacy such as α- amylase inhibition activity was assessed through the following protocols: Alpha-amylase was diluted in 5 mL of 5 mM phosphate buffer (pH 6.9) to a concentration of 1 Units/mL for the alpha-amylase inhibition experiment. Starch was boiled to a clear solution in 5 mM phosphate-buffered saline (pH 6.8). The chromogenic non-pre-incubation technique was used; it was derived from Sigma-Aldrich. 40 microtiters of cAP-CNP, bare CNP, and plant extract were combined in separate sets of experiments with 160 µL of distilled water and 400 µL of starch solution in screw-cap plastic tubes, which was then incubated for 45 minutes at room temperature. Following incubation, 20 µL of the mixture and 10 µL of DNS color reagent were transferred to a different test tube. Nanodrop was used to assess the absorbance at 540 nm after heating it for 90 minutes and diluted with water (Mechchate *et al.*, 2021a; Liu *et al.*, 2013; Mechchate *et al.*, 2021b).

2.6. Cellular biocompatibility and anti-inflammatory assessment

The HaCat cell line was used for the MTT-based biocompatibility assay of the cAP-CNP sample. At first, 5,000 cells were placed in each well of a 96-well plate and incubated at a temperature of 37ºC in a 5% CO_2 incubator for 48 hours. To guarantee repeatability, a total of five measurements were conducted. Following a 48-hour incubation period, cAP-CNP was administered to each well at a concentration of 5mg/ml, followed by the addition of 5mg/ml MTT reagent. The plate was reinserted into the incubator for a further 4 hours. Next, the MTT

solution was extracted, and 100 µL of DMSO was introduced to each well to delicately dissolve the Formazan crystals. The measurements were taken at a wavelength of 570 nm, and the cell viability percentage was calculated. Human monocyte-derived cells were cultured and maintained using a solution of 100 U/ml penicillin-streptomycin (antibiotics) and 10% FBS-containing RPMI media. The cells were kept at a temperature of 37ºC in an incubator with a 5% concentration of carbon dioxide. Subsequently, the cells were subjected to a 24-hour stimulation with lipopolysaccharides (LPS) at a concentration of 100 ng/ml to induce the production of inflammatory cytokines. Subsequently, the impact of medicines on cytokine production was assessed by subjecting the cells to medium control and drug concentrations of 250 g/ml (cAP-CNP, IC50 conc.) for 24 hours. The cells were subsequently subjected to RNA extraction using Sigma Aldrich's Trizol reagent, following the manufacturer's instructions. The extracted RNA was then converted into cDNA using the Aurea cDNA synthesis kit, following the manufacturer's instructions. Finally, real-time PCR-based gene expression analysis was performed to measure the levels of two inflammatory cytokines, TNF-alpha and IL-6. The forward primer for TNF alpha is CCTCTCTCTAATCAGCCCTCTG, and the reverse primer is GAGGACCTGGGAGTAGATGAG. The forward primer for IL-6 is ACTCACCTCTTCAGAACGAATTG, and the reverse primer is CCATCTTTGGAAGGTTCAGGTTG. The β-actin gene is often used as a housekeeping gene. The relative gene expression data was assessed using the ddCt technique in qPCR.

3. RESULTS

3.1 Synthesis and characterization of cAP-CNP

Crude *Andrographis paniculata* and Cerium oxide nanoparticle (cAP-CNP) conjugate were successfully synthesized using the protocols of green chemistry using the crude phytoconstituents obtained from the plant via Soxhlet apparatus acting as the oxidizer as well as stabilizing agent in the synthesis of conjugated nanomaterial. cAP-CNP conjugate nanomaterial after calcination was subjected to characterization for further studies. The primary confirmation of conjugation was done with UV-visible spectroscopy where the range of absorbance obtained at 310 nm showed the oxidation state of Ce^{4+} (Fig. 1a), the particle size of the obtained nanomaterial was confirmed by the Dynamic Light Scattering Analysis which showed a hydrodynamic radius of 100 nm for bare CNP and after conjugation with crude *Andrographis paniculata* it showed a hydrodynamic radius of 150 nm (Fig. 1b) which further confirmed the conjugation on the surface of CNP. The surface morphology after conjugation of nanomaterial was studied through Scanning Electron Microscopy (Fig. 2a). X-ray Diffraction analysis was also studied to define the presence of crystals in cAP-CNP conjugate and the peaks obtained in XRD clearly show the confirmatory peak at 111, 200, 211, 311-crystal planes. The presence of functional groups on the surface of CNP-Ap conjugate was studied through FTIR analysis, which indicated the signature peaks of both bare CNP and *Andrographis paniculata* crude extract (Fig. 3).

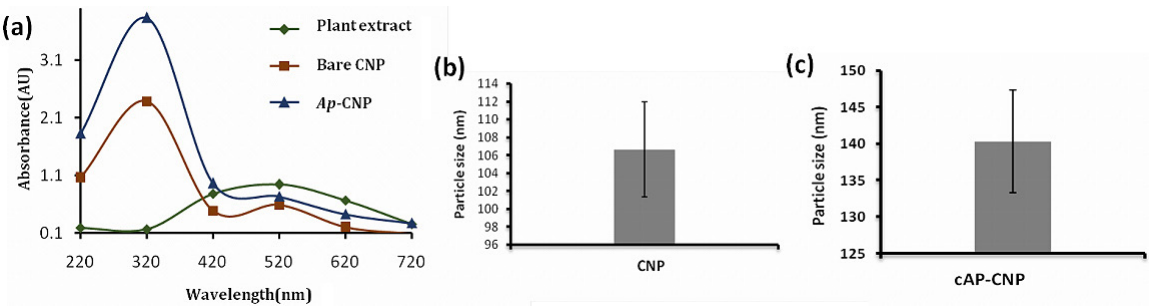

Figure 1. a) Represents the UV-visible characterization of the bare CNP and cAP-CNP synthesized nanomaterials. b) and c) the Dynamic Light Scattering characterization for the size analysis of synthesized cerium oxide nanoparticles.

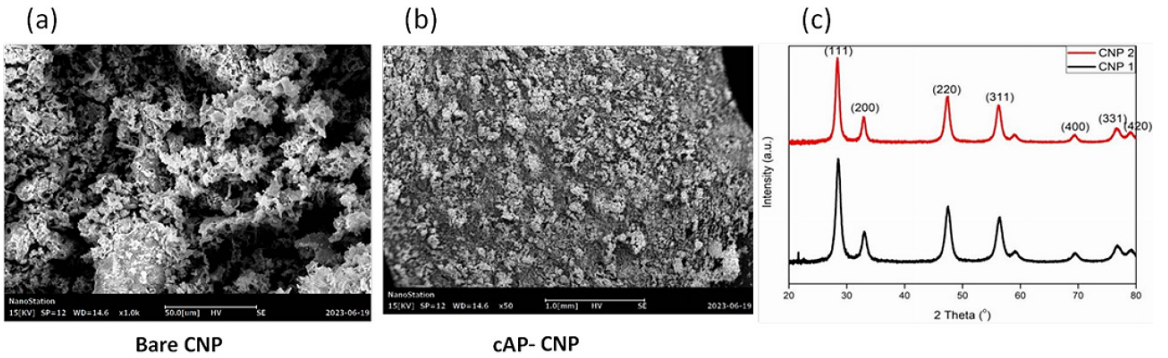

Figure 2. Scanning Electron Microscope (SEM)and X-ray Diffraction (XRD) analysis of the synthesized cerium oxide nanomaterials. a and b) the SEM image of the ultrafine powder of synthesized bare CNP and cAP- CNP. c) The XRD graph obtained for the bare CNP and cAP-CNP nanoparticles respectively.

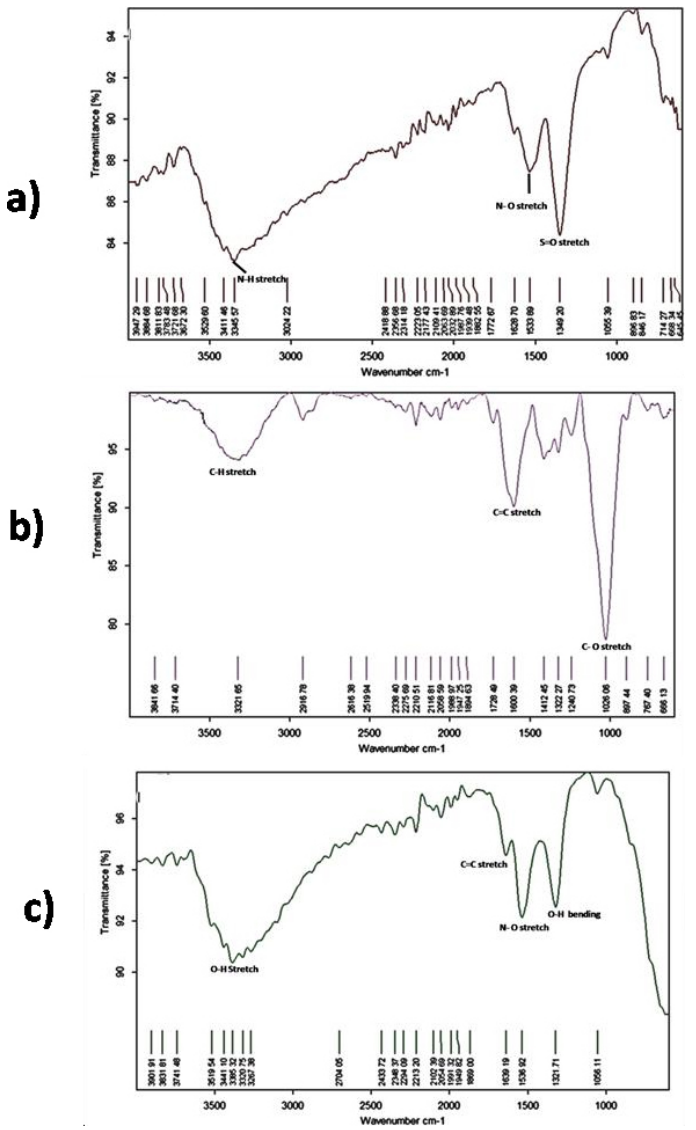

Figure 3. FTIR spectra of the a) bare CNP, b) crude plant extract of *Andrographis paniculata* and c) cAP-CNP.

3.2. Antioxidative Reactive Oxygen Species (ROS) scavenging analysis

The antioxidative efficiency of synthesized cAP-CNP conjugate was evaluated using biochemical assays for each catalase and SOD mimetic activity. Catalase mimetic activity was assessed via biochemical assay in which the H_2O_2 degradation parameters were measured and it was observed that the crude plant extract of *Andrographis paniculata*, bare CNP and cAP-CNP conjugate showed a varying range of scavenging activity (Fig. 4). The crude plant extract showed a lower range of H_2O_2 scavenging activity in comparison to bare CNP which showed moderate H_2O_2 scavenging activity of 27.8% whereas due to the synergistic effect of conjugation of the cAP-CNP conjugateshowed an enhanced activity of 61.4%. The H_2O_2 scavenging activity was directly proportional to the concentration of cAP-CNP conjugate sample used (Fig. 4c, d).

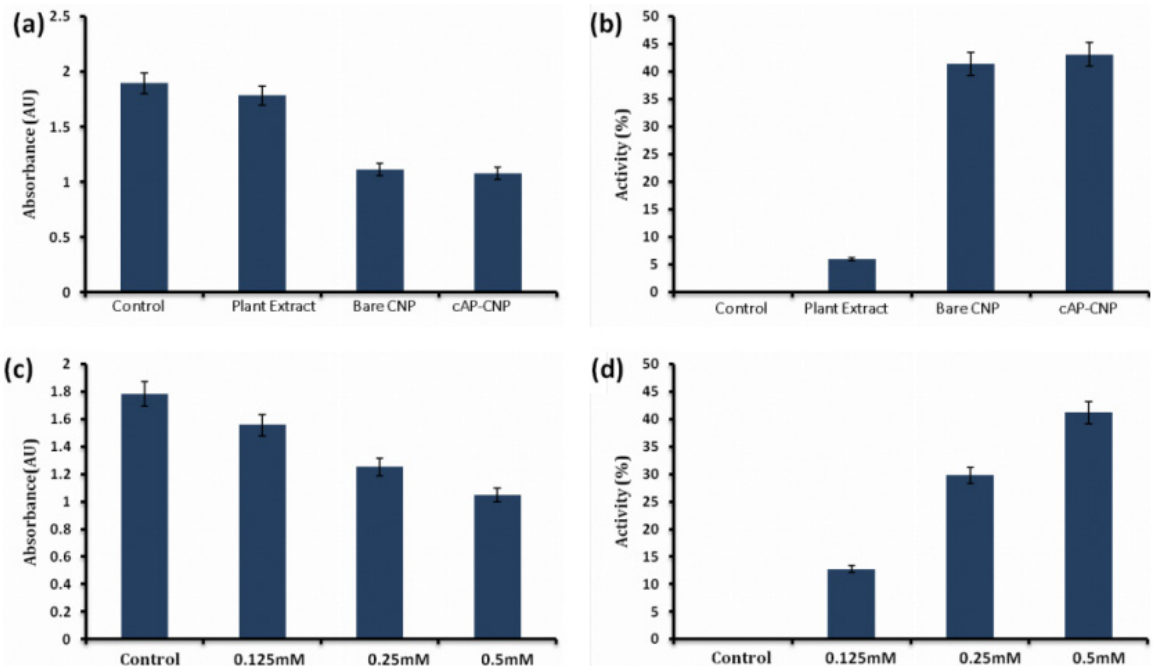

Figure 4. The Catalase mimetic activity of synthesized cAP-CNP nanomaterials. Catalase mimetic assay demonstrated the H_2O_2 scavenging activity of all samples at different concentrations. a) The absorption of the samples-Plant extract, bare CNP and cAP-CNP in comparison with H_2O_2 (control), b) The percentage scavenging activity of samples in comparison to the control; c, d) absorption and percentage scavenging activity respectively of different concentrations. All the experiments were performed in triplicate and the data are presented in the form of Mean± S.D.

For studying the SOD mimetic activity of the cAP-CNP conjugate, Nitrobule Tetrazolium (NBT) reduction assay was done using riboflavin-methionine mediated superoxide radical generation. All three sets of samples i.e, plant extract, bare CNP and cAP-CNP conjugate were used and it was observed that plant extract showed a lower range of activity in comparison to bare CNP which showed an activity range of 41.33% and cAP-CNP conjugate showed a range of 43.03% activity (Fig. 5). The SOD activity was also established to be directly proportional to the concentration of cAP-CNP conjugate (Fig. 5c, d).

3.3. Anti-microbialanalysis of cAP-CNP conjugate

To evaluate the anti-microbial efficacy of cAP-CNP conjugate, a Minimum Inhibitory Concentration (MIC) assay was carried out using 10^6 folds concentration of *E. coli*. It was observed that the anti-microbial activity of cAP-CNP conjugate was enhanced by the synergistic effects of conjugation as the antimicrobial potential of crude extract of *Andrographis paniculata* was observed to be around 18%, the antimicrobial efficacy of bare CNP was around 45.8% which was moderate activity rate but

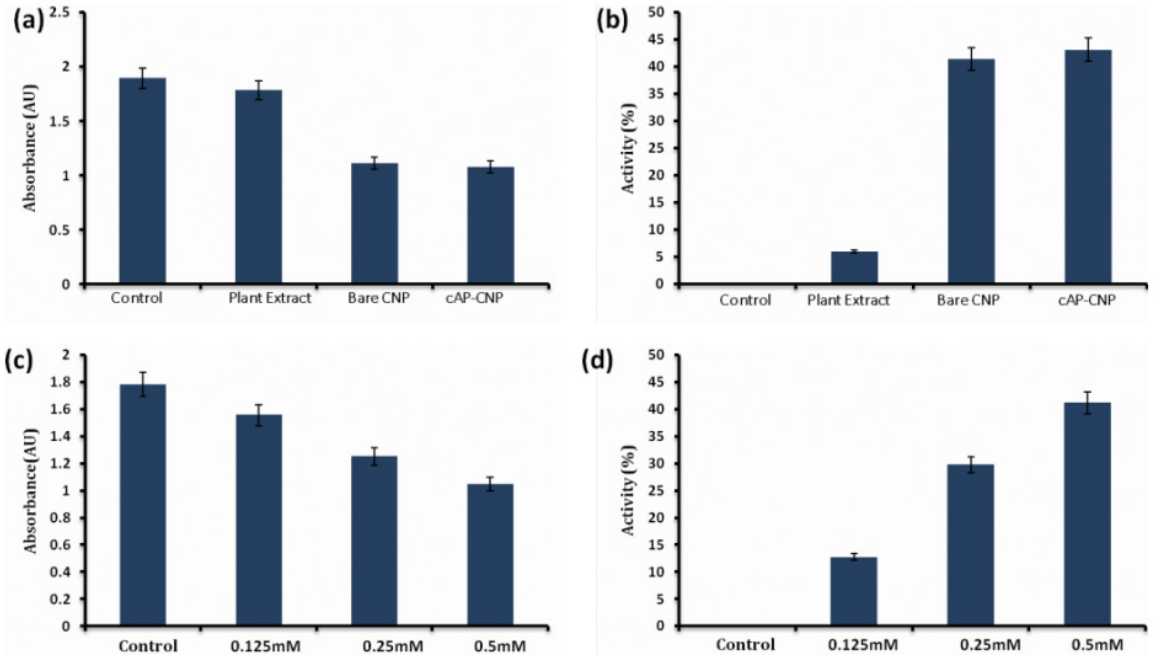

Figure 5. The superoxide dismutase mimetic activity of synthesized cAP-CNP nanomaterials, bare CNP and crude plant extract of *Andrographis paniculata*. Superoxide Dismutase mimetic assay demonstrated the superoxide ions scavenging activity of all samples. a) Absorption of all the samples- Plant extract, bare CNP and cAP-CNP in comparison with control. b) The percentage Inhibition of all samples in comparison to the control. c) and d) absorption and percentage inhibition respectively of cAP-CNP at different concentrations. All the experiments were performed in triplicate and the data are presented in the form of Mean± S.D.

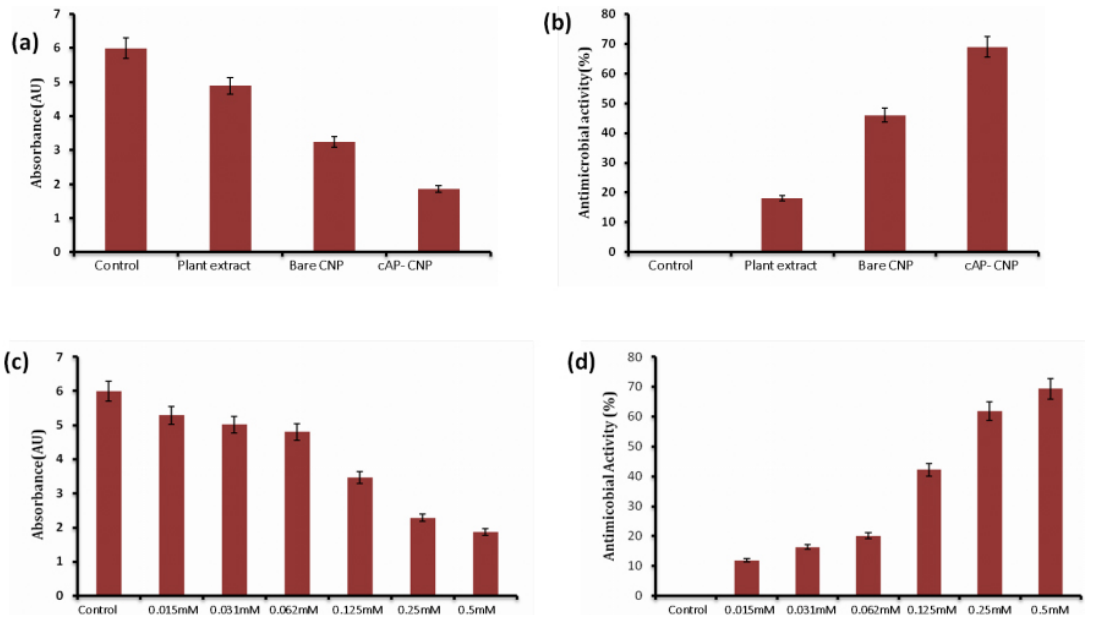

Figure 6. The antimicrobial efficiency of different samples against 10^6 folds *E. coli* Culture. a)The absorption of different samples- plant extract, bare CNP and cAP-CNP in comparison with control treatment. b)The percentage inhibition of the different samples in comparison to the control treatment. c and d) The absorption and percentage inhibition of cAP-CNP at different concentrations. All the experiments were performed in triplicate and the data are presented in the form of Mean± S.D.

due to the synergistic effects of conjugation, it was enhanced up to 68.9% (Fig. 6). The antimicrobial activity of cAP-CNP conjugate was directly proportional to the nanoparticle concentration (Fig. 6c, d).

3.4. α-Amylase degradation analysis of cAP-CNP conjugate

The biochemical assay of α-Amylase inhibition analysis was done as a proof of concept for the anti-diabetic properties of cAP-CNP conjugate. It was observed that the crude plant extract showed inhibition activity for α- amylase up to 63% due to the reported potential of *Andrographis paniculata* as a potent anti-diabetic compound in comparison to bare CNP which showed inhibition activity up to 43% whereas the cAP-CNP conjugate showed enhanced inhibitory activity for α-amylase up to 86.8% due to synergistic effects (Fig. 7). By varying the concentration of samples in a series of experiments it was observed that the α- amylase inhibition activity of cAP-CNP was directly proportional to the concentration that is with an increase in the concentration of cAP-CNP conjugate, the activity of α- amylase inhibition was increased (Fig. 7c, d). Hence it can be observed that due to the optimizations of the conjugation chemistry, the efficacy can be improvised to a higher percentage. α- amylase is secreted through the pancreatic cells in the human body and is responsible for breaking down complex carbohydrates into simpler ones such as Glucose. Hence, the inhibition in the activity of α- amylase will result in lowering the level of free glucose in blood, in the biochemical assay for assessment of inhibition activity.

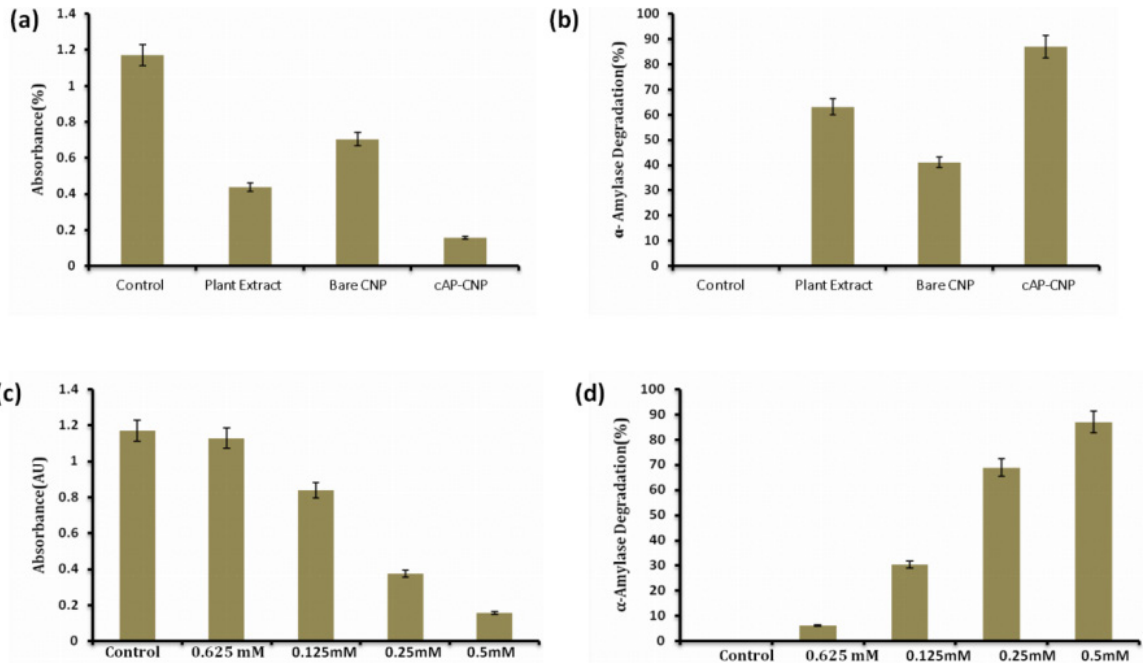

Figure 7. The α-amylase inhibition efficiency of the different nanomaterials treated. a)The absorption of the samples- plant extract, bare CNP and cAP-CNP in comparison with the control treatment. b) The percentage Inhibition of the samples in comparison to the control treatment. c,d) absorption and percentage Inhibition respectively of cAP-CNP at different concentrations All the experiments were performed in triplicate and the data are presented in the form of Mean± S.D.

3.5. Cellular biocompatibility and anti-inflammatory assessment

The biocompatibility of cAP-CNP was evaluated using the HaCat cell line, which is a human skin keratinocyte cell line. The experiment included using cAP-CNP solutions with various concentrations, namely 0.5 µM, 0.25 µM, 0.125 µM, and 0.0625 µM. Following the treatment, post-treatment MTT research was done to assess the effects on biocompatibility. The results of the investigation demonstrated that the synthesized cAP-CNP displayed cellular biocompatibility. The cellular viability levels of HaCat cells treated with cAP-CNP at a dose of 0.5 µM

were around 84.6%, suggesting that it is not hazardous. The outcomes of the biocompatibility study performed at various concentrations were assessed. The Anti-inflammatory test used U937 cells, which are generated from human monocytes. These cells were cultured and maintained in RPMI medium with 10% FBS and 100 U/ml of penicillin-streptomycin antibiotics. The activity was determined by measuring the decrease in expression of TNF-α and IL-6. The synthesized cAP-CNP demonstrated anti-inflammatory activity by lowering the expression of IL-6 (Interleukin-6) and TNF-α to 89% and 81% respectively.

4. DISCUSSION

The field of nanotechnology has seen significant growth, with numerous applications in various sectors. Nanoparticles (NPs) are of particular importance due to their unique physical and chemical attributes, despite their small size ranging from 1-100 nm. Particles at the nanoscale have improved capabilities in catalysis, mechanics, chemistry, and biology (Ramos *et al.,* 2017). Their high surface-to-volume ratio makes them highly reactive and mobile, with excellent dissolving abilities and strength. NPs are produced through various techniques, and they occur naturally on Earth in sources like soil, water, volcanic dust, and minerals. Different industries, such as food and beverages, agriculture, and pharmaceuticals sectors utilize nanoparticles. Researchers worldwide are showing significant interest in using nanoparticles in biocompatible materials to create hybridized scaffolds (Kaushik, 2019). Among these nanoparticles, cerium has been synthesized in various ways, but the use of green chemistry principles offers a simpler and more eco-friendly approach. Crude *Andrographis paniculata* (Ap) and Cerium oxide Nanoparticles (CNP) conjugated together have shown beneficial synergistic effects, especially in the activities of cAP-CNP conjugate. The confirmation of conjugation was done through different physiochemical characterization techniques – the primary confirmation was done through UV-visible spectroscopy (Fig. 1a) as seen in the figure, the major peaks were obtained at 310nm showing the predominant presence of Ce^{4+} oxidation state. According to previously published reports, a higher Ce^{+4}/Ce^{+3} oxidation state shows significantly higher Catalase mimetic activity rather than Superoxide dismutase mimetic activity (Singh *et al.,* 2021). The hydrodynamic radius of conjugated nanomaterial and bare CNP was confirmed by the Dynamic Light Scattering (DLS) technique and the radius parameters were found by the previous reports (Singh *et al.,* 2018). Through the difference of radius in bare CNP and cAP-CNP can be concluded that there was successful conjugation of materials as the radius of bare CNP increased from 106 nm to 140 nm and their size range corresponds to the defined nano-scale parameter (Fig. 1b). The hydration radius of cAP-CNP conjugate was expected to increase as compared to bare CNP with addition of phytoconstituents of Crude *Andrographis paniculata.* The surface morphology was studied through SEM and at the resolution of 1mm the cAP-CNP conjugate can be seen (Fig. 2a). Further, XRD analysis confirmed the crystallinity of the nanomaterials through the signatory cerium peaks obtained at crystal planes 111, 200, 220 and 311 the crystalline nature of the synthesized nanomaterial was assessed concerning the previously reported work and the data shows that the bare CNP has 98 % crystallinity whereas cAP-CNP was 91.8% (Ghanbary & Jafarnejad, 2017) (Fig. 2b). To confirm the presence of active compounds and fingerprinting compounds of all the synthesized nanomaterials FTIR was done and it was concluded regarding the reported literature that the signatory peaks of functional group present in *Andrographis paniculata* (Sangeetha *et al.,* 2014) crude extract such as Alkene=C-H bending at 894.6nm, Amine C-H stretching at 1409.96nm, Aromatic C-C stretch at 1543.05nm. and bare CNP such as Hydroxyl group at 3300 nm, Amide group at 1640 nm, and O-H bending at 1204 nm. (Farahmandjou *et al.,* 2016) were present in the conjugated Nanomaterial cAP-CNP- Alkene=C-H bending at 894.6nm, Amine C-H stretching at 1409.96nm, O-H bending at 1204 nm, Hydroxyl group at 3300 nm (Fig. 3).

As shown in Fig. 4, cAP-CNPcatalase mimetic activity was up to twice as strong as that of bare CNP. As it is evident from the graph the Catalase mimetic activity of plant extract was 6.24%, bare CNP was 27.8% and conjugated nanomaterial cAP-CNP was 61.4%. This improvement in activity suggests that conjugating CNP with crude plant extracts contains bioactive components which might considerably increase its anti-oxidative ability. This enhanced property can be of immense significance (Pirmohamed *et al.,* 2010; Singh *et al.,* 2012) as mentioned above the catalase mimetic activity is predominantly seen in the oxidation state of Ce^{4+}

which was confirmed through the absorption peak of 310nm. Additionally, this conjugation moderately increased the Superoxide Dismutase (SOD) mimetic activity. It was observed in the graph that Plant extract was 5.9 % Bare CNP was 41.33% and conjugated Nanomaterial cAP-CNP was 43%, which might be further optimized to get even better outcomes (Korsvik *et al.,* 2007; Singh *et al*., 2013).

Additionally, cAP-CNP's biological characteristics were improved in a number of ways. *Andrographis paniculata* contains phenols, terpenoids, and flavonoids which have bioactive properties. The antibacterial activity increased up to 1.5-fold, as shown in Fig. 6. The antibacterial activity of Plant extract was 18 %, bare CNP was 45.9% and conjugated Nanomaterial cAP-CNP was 68.95% (Zhang *et al.,* 2019). Cerium oxide nanoparticle dual oxidative states of Ce^{+4}/Ce^{+3} ratio reduce the production of free radicals and cause modifications in the membrane structure of bacterial cell walls, both of which have an antimicrobial effect. These two strong chemicals may be conjugated to increase the biological effectiveness of their combined actions (Estes *et al.,* 2021). Fig. 7 illustrates the improvement in α-amylase inhibition activity, which serves to further emphasize the advantages of conjugation in the anti-diabetic significance of Biomaterial. The α-amylase enzyme secreted by the pancreatic cells helps in the degradation of complex carbohydrates into simpler forms such as Glucose. The inhibition of α-amylase activity will ultimately lead to the regulation of free glucose levels resulting in controlled free glucose in blood. It was observed that the α-amylase inhibition activity of Plant extract was 63% due to the reported properties of *Andrographis paniculata*, bare CNP was 41% whereas due to the synergistic effects of conjugation, the inhibition efficacy of cAP-CNP was 86.8%. The obtained values were assessed based on the reported literature (Wickramaratne *et al.,* 2016). Fig. 8 illustrates the *In-vitro* assessment results of cAP-CNP at different concentrations for the biocompatibility and anti-inflammatory roles. A post-treatment MTT study evaluated the impact on biocompatibility. The observations demonstrated that the synthesized cAP-CNP conjugates exhibited cellular biocompatibility. The cellular viability of HaCat cells treated with cAP-CNP at a concentration of 0.5 µM was around 84.6%, indicating that it is not harmful. The results of the biocompatibility research conducted at different doses were evaluated. The anti-inflammatory test used U937 cells, derived from human monocytes. The activity was assessed by quantifying the reduction in the expression of TNF-α and IL-6. As TNF-α and IL-6 are cytokines released during the event of inflammation in the body a reduction in the level of these cytokines reveals the potential of cAP- CNP to lower the amount of inflammation in cell lines after treatment. The synthesized cAP-CNP exhibited anti-inflammatory properties by reducing the expression of IL-6 (Interleukin-6) and TNF-α by 89% and 81% respectively. The above analysis was cross-referred with the reported literature (Kalyanaraman *et al*., 2019; Hirst *et al.,* 2009). Herein, our hypothesis for the work done is due to the active presence of bioactive compounds in the crude extract of *Andrographis paniculata* obtained via Soxhlet apparatus and bare CNP having inherent strong antioxidative properties due to dual oxidation state of Ce^{3+} and Ce^{4+}. The positive synergism of conjugation between the above two components resulted in enhanced reported properties of *Andrographis paniculate* and Cerium oxide Nanoparticles. This proof of concept for positive synergism will be the scaffold for us to look out for better prospects of this conjugated nanomaterial cAP-CNP as a next-generation therapeutic compound. As this conjugation is not been reported yet researchers may examine the potential of *Andrographis paniculata* and cerium oxide nanoparticles (cAP-CNP) for a range of therapeutic applications by using the improved characteristics and biological efficacy obtained via their conjugation. The promising findings of this study provide a viable foundation for our futuristic and mechanistic investigation into identifying the specific and signature phytoconstituents from *Andrographis paniculate* and synergistic role.

5. CONCLUSION

We report for the first time, the sustainable fabrication of cerium oxide nanomaterials using the crude extracts of *Andrographis paniculate* plant. The process leads to enhanced development of redox-active cerium oxide nanomaterial with excellent antioxidative reactive oxygen scavenging properties. This synergism also leads to prospective application into the antimicrobial arena for the utilization of synthesized nanomaterials, as evident from the obtained data. Further to our surprises, the findings have identified the potential role of the synthesized cAP-CNP conjugates in the anti-diabetic and towards being the anti-inflammatory zone with its decrease in

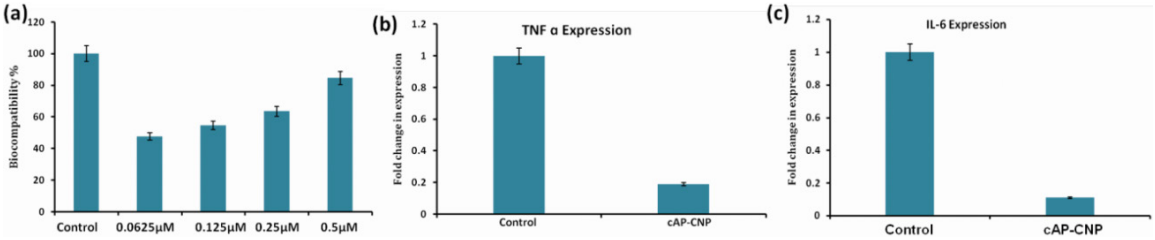

Figure 8. The Biocompatibility and Anti-inflammatory Efficiency of cAP-CNP. a) The Biocompatibility percentage of cAP-CNP at different concentrations;b) folds of changes observed in TNF- α expression level in comparison to the control treatment. c)The folds of changes observed in IL-6 expression level in comparison to the control treatment. All the experiments were performed in triplicates and the data are presented in the form of Mean± S.D.

alpha-amylase activity and reducing the expression of TNF-alpha and IL-6 factors. We highly anticipate that future pharmaceutical research will benefit immensely from these findings towards sensitizing drug development for biomedical perspectives.

Declaration

Ethical Approval – N.A

Funding

We acknowledge the DST-Science and Engineering Research Board (Start-up Research Grant Scheme), Govt. of India for the funding support. File no. SRG_2022_000237

Availability of data and materials

Information on data and materials will be accessible on the solicitation from authors. ♦

REFERENCES

Aseyd Nezhad, S., Es-haghi, A., & Tabrizi, M. H. (2020). Green synthesis of cerium oxide nanoparticle using Origanum majorana L. leaf extract, its characterization and biological activities. Applied Organometallic Chemistry, 34(2), e5314.

Cheung, H. Y., Cheung, C. S., & Kong, C. K. (2001). Determination of bioactive diterpenoids from Andrographis paniculata by micellar electrokinetic chromatography. Journal of Chromatography A, 930(1-2), 171-176.

Chien, C. F., Wu, Y. T., Lee, W. C., Lin, L. C., & Tsai, T. H. (2010). Herb–drug interaction of Andrographis paniculata extract and andrographolide on the pharmacokinetics of theophylline in rats. Chemico-biological interactions, 184C3), 458-465.

Estes, L. M., Singha, P., Singh, S., Sakthivel, T. S., Garren, M., Devine, R., ... & Handa, H. (2021). Characterization of a nitric oxide (NO) donor molecule and cerium oxide nanoparticle (CNP) interactions and their synergistic antimicrobial potential for biomedical applications. Journal of colloid and interface science, 586, 163-177.

Farahmandjou, M., Zarinkamar, M., & Firooz-abadi, T. P. (2016). Synthesis of Cerium Oxide (CeO2) nanoparticles using simple CO-precipitation method. Revista mexicana de física, 62(5), 496-499.

Gahlaut, A., & Chhillar, A. K. (2013). Evaluation of antibacterial potential of plant extracts using resazurin based microtiter dilution assay. International Journal of Pharmacy and Pharmaceutical Sciences, 5(2), 372-376.

Ghanbary, F., & Jafarnejad, E. (2017). Removal of malachite green from the aqueous solutions using polyimide nanocomposite containing cerium oxide as adsorbent. Inorganic and Nano-Metal Chemistry, 47(12), 1675-1681.

Hirst, S. M., Karakoti, A. S., Tyler, R. D., Sriranganathan, N., Seal, S., & Reilly, C. M. (2009). Anti-inflammatory properties of cerium oxide nanoparticles. Small, 5(24), 2848-2856.

Ivanova, E., Atanasova-Pančevska, N., & Kungulovski, D. (2013). Antimicrobial activities of laboratory produced essential oil solutions against five selected fungal strains. Zbornik Matice srpske za prirodne nauke, (124), 171-183.

Javadi, F., Yazdi, M. E. T., Baghani, M., & Es-haghi, A. (2019). Biosynthesis, characterization of cerium oxide nanoparticles using Ceratonia

siliqua and evaluation of antioxidant and cytotoxicity activities. Materials Research Express, 6(6), 065408.

Kalyanaraman, V., Naveen, S. V., Mohana, N., Balaje, R. M., Navaneethakrishnan, K. R., Brabu, B., … & Kumaravel, T. S. (2019). Biocompatibility studies on cerium oxide nanoparticles–combined study for local effects, systemic toxicity and genotoxicity via implantation route. Toxicology research, 8(1), 25-37.

Karuppusamy, S., & Rajasekaran, K. M. (2009). High throughput antibacterial screening of plant extracts by resazurin redox with special reference to medicinal plants of Western Ghats. Global Journal of Pharmacology, 3(2), 63-68.

Kaushik, A. (2019). Biomedical nanotechnology related grand challenges and perspectives. Frontiers in Nanotechnology, 1, 1.

Khatami, M., Sarani, M., Mosazadeh, F., Rajabalipour, M., Izadi, A., Abdollahpour-Alitappeh, M., ... & Borhani, F. (2019). Nickel-doped cerium oxide nanoparticles: green synthesis using stevia and protective effect against harmful ultraviolet rays. Molecules, 24(24), 4424.

Korsvik, C., Patil, S., Seal, S., & Self, W. T. (2007). Superoxide dismutase mimetic properties exhibited by vacancy engineered ceria nanoparticles. Chemical communications, (10), 1056-1058.

Liu, J., Hay, J., & Faught, B. E. (2013). The association of sleep disorder, obesity status, and diabetes mellitus among US adults—The NHANES 2009-2010 survey results. International journal of endocrinology, 2013.

Mechchate, H., Es-Safi, I., Haddad, H., Bekkari, H., Grafov, A., & Bousta, D. (2021). Combination of Catechin, Epicatechin, and Rutin: Optimization of a novel complete antidiabetic formulation using a mixture design approach. The Journal of Nutritional Biochemistry, 88, 108520.

Mechchate, H., Es-Safi, I., Louba, A., Alqahtani, A. S., Nasr, F. A., Noman, O. M., ... & Bousta, D. (2021). In vitro alpha-amylase and alpha-glucosidase inhibitory activity and in vivo antidiabetic activity of Withania frutescens L. Foliar extract. Molecules, 26(2), 293.

Mendes, R. H., Hagen, M. E. K., Barp, J., Jong, E. V. D., Moreira, J. D., Oliveira, Á. R. D., ... & Bellló-Klein, A. (2014). Isolated soy protein-based diet ameliorates glycemia and antioxidants enzyme activities in streptozotocin-induced diabetes. Food and Nutrition Sciences. Irvine, CA. Vol. 5, n. 21 (Nov. 2014), p. 2089-2096.

Miri, A., & Sarani, M. (2018). Biosynthesis, characterization and cytotoxic activity of CeO2 nanoparticles. Ceramics International, 44(11), 12642-12647.

Pirmohamed, T., Dowding, J. M., Singh, S., Wasserman, B., Heckert, E., Karakoti, A. S., ... & Self, W. T. (2010). Nanoceria exhibit redox state-dependent catalase mimetic activity. Chemical communications, 46(16), 2736-2738.

Ramos, A. P., Cruz, M. A., Tovani, C. B., & Ciancaglini, P. (2017). Biomedical applications of nanotechnology. Biophysical reviews, 9(2), 79-89.

Sangeetha, S., Archit, R., & Sathia Velu, A. (2014). Phytochemical testing, antioxidant activity, HPTLC and FTIR analysis of antidiabetic plants Nigella sativa, Eugenia jambolana, Andrographis paniculata and Gymnema sylvestre. J. Biotechnol, 9, 1-9.

Saxena, R. C., Singh, R., Kumar, P., Yadav, S. C., Negi, M. P. S., Saxena, V. S., ... & Amit, A. (2010). A randomized double blind placebo controlled clinical evaluation of extract of Andrographis paniculata (KalmCold™) in patients with uncomplicated upper respiratory tract infection. Phytomedicine, 17(3-4), 178-185.

Singh, R., Karakoti, A. S., Self, W., Seal, S., & Singh, S. (2016). Redox-sensitive cerium oxide nanoparticles protect human keratinocytes from oxidative stress induced by glutathione depletion. Langmuir, 32(46), 12202-12211.

Singh, S., Kumar, U., Gittess, D., Sakthivel, T. S., Babu, B., & Seal, S. (2021). Cerium oxide nanomaterial with dual antioxidative scavenging potential: Synthesis and characterization. Journal of Biomaterials Applications, 36(5), 834-842.

Singh, S., Ly, A., Das, S., Sakthivel, T. S., Barkam, S., & Seal, S. (2018). Cerium oxide nanoparticles at the nano-bio interface: Size-dependent cellular uptake. Artificial Cells, Nanomedicine, and Biotechnology, 46(sup3), 956-963.

Singh, S., Singh, A. N., Verma, A., & Dubey, V. K. (2013). A novel superoxide dismutase from Cicer arietinum L. seedlings: isolation, purification and characterization. Protein and peptide Letters, 20(7), 741-748.

Singh, S., Verma, A., & Dubey, V. K. (2012). Effectivity of anti-oxidative enzymatic system on diminishing the oxidative stress induced by aluminium in chickpea (Cicer arietinum L.) seedlings. Brazilian Journal of Plant Physiology, 24, 47-54.

Smith, H. J., Milberg, S. J., & Burke, S. J. (1996). Information privacy: Measuring individuals' concerns about organizational practices. MIS quarterly, 167-196.

Weydert, C. J., & Cullen, J. J. (2010). Measurement of superoxide dismutase, catalase and glutathione peroxidase in cultured cells and tissue. Nature protocols, 5(1), 51-66.

Wickramaratne, M. N., Punchihewa, J. C., & Wickramaratne, D. B. M. (2016). In-vitro alpha amylase inhibitory activity of the leaf extracts of Adenanthera pavonina. BMC complementary and alternative medicine, 16, 1-5.

Wu, D., Cao, X., & Wu, S. (2012). Overlapping elution–extrusion counter-current chromatography: A novel method for efficient purification of natural cytotoxic andrographolides from Andrographis paniculata. Journal of Chromatography A, 1223, 53-63.

Zhang, M., Zhang, C., Zhai, X., Luo, F., Du, Y., & Yan, C. (2019). Science China Materials, 62, 1727-1739.

Zou, Q. Y., Li, N., Dan, C., Deng, W. L., Peng, S. L., & Ding, L. S. (2010). A new ent-labdane diterpenoid from Andrographis paniculata. Chinese Chemical Letters, 21(9), 1091-1093.